Small-Strain Stiffness, Shear-Wave Velocity, and Soil Compressibility

Minsu Cha, Ph.D., A.M.ASCE[1]; J. Carlos Santamarina, Ph.D., M.ASCE[2]; Hak-Sung Kim[3]; and Gye-Chun Cho, Ph.D.[4]

Abstract: The small-strain shear modulus depends on stress in uncemented soils. In effect, the shear-wave velocity, which is often used to calculate shear stiffness, follows a power equation with the mean effective stress in the polarization plane $V_s = \alpha(\sigma'_m/1\ \text{kPa})^{\beta}$, where the α factor is the velocity at 1 kPa, and the β exponent captures the velocity sensitivity to the state of stress. The small-strain shear stiffness, or velocity, is a constant-fabric measurement at a given state of stress. However, parameters α and β are determined by fitting the power equation to velocity measurements conducted at different effective stress levels, so changes in both contact stiffness and soil fabric are inherently involved. Therefore, the α and β parameters should be linked to soil compressibility C_C. Compiled experimental results show that the α factor decreases and the β exponent increases as soil compressibility C_C increases, and there is a robust inverse relationship between α and β for all sediments: $\beta \approx 0.73 - 0.27 \log[\alpha/(\text{m/s})]$. Velocity data for a jointed rock mass show similar trends, including a power-type stress-dependent velocity and inverse correlation between α and β; however, the α-β trend for jointed rocks plots above the trend for soils. **DOI: 10.1061/(ASCE)GT.1943-5606.0001157.** © *2014 American Society of Civil Engineers.*

Author keywords: Shear-wave velocity; Velocity-stress power relations; Contact effects; Compression index; Granular fabric; Coordination number.

Introduction

Soils and fractured rocks are granular materials. The small-strain shear stiffness G reflects contact-level deformation and exhibits a Hertzian-type power relation with effective stress. Shear-wave propagation is the most versatile and portable method to assess the small-strain shear stiffness in the laboratory (e.g., bender element and resonant column) and in the field (e.g., cross hole, seismic cone, and surface waves). The shear-wave velocity V_S (m/s) is determined by the mean effective stress in the polarization plane σ'_m (kPa) (Hardin and Drnevich 1972; Knox et al. 1982; Petrakis and Dobry 1987; Santamarina and Cascante 1996)

$$V_S = \sqrt{\frac{G}{\rho}} = \alpha \left(\frac{\sigma'_{\perp} + \sigma'_{//}}{2\ \text{kPa}} \right)^{\beta} \tag{1}$$

where $\sigma'_{\perp}$ and $\sigma'_{//}$ = effective stresses in the direction of particle motion and the direction of wave propagation, respectively; the α factor (m/s) = shear-wave velocity at a mean effective stress $\sigma'_m = 1$ kPa; and the β exponent captures the sensitivity of the skeletal shear stiffness to the applied stress. This equation applies when capillary forces are significantly smaller than stress-induced skeletal forces.

Although wave propagation is a small-strain constant-fabric stiffness measurement, velocity-stress relations such as Eq. (1) are fitted to wave-velocity data gathered at different effective stress levels that inherently involve fabric changes. Therefore, the velocity-stress power relationship captures both contact behavior and fabric changes. [Note that the correction factor for void ratio e frequently used in other forms of Eq. (1) is implicitly included in the α factor (Hardin and Richart 1963; Hardin and Drnevich 1972; Lo Presti et al. 1995; Shibuya et al. 1997).]

Soil compressibility C_C measured in oedometer cells is primarily the result of interparticle relative displacement and fabric changes. Thus, a causal link between small-strain α and β parameters and the compressibility C_C of soils is anticipated. The authors compiled a database to explore relations between these parameters; the database includes a wide range of soils, from fine to coarse, both natural and freshly remolded specimens, and both normally and overconsolidated sediments.

Compressibility and Shear-Wave Velocity

The sediment compressibility for a normally consolidated soil can be characterized using the compression index C_C obtained by fitting the standard void ratio e versus vertical effective stress σ'_z relation to laboratory data

$$e = e_0 - C_C \log\left(\frac{\sigma'_z}{\sigma'_{z0}}\right) \tag{2}$$

Fig. 1 shows the correlation between the α factor and β exponent with compressibility. Data are collected from previous studies

[1]Postdoctoral Fellow, School of Civil and Environmental Engineering, Georgia Institute of Technology, Atlanta, GA 30332-0355 (corresponding author). E-mail: mcha678@gmail.com

[2]Professor, School of Civil and Environmental Engineering, Georgia Institute of Technology, Atlanta, GA 30332-0355. E-mail: jcs@gatech.edu

[3]Doctoral Candidate, Dept. of Civil and Environmental Engineering, Korea Advanced Institute of Science and Technology (KAIST), Yuseong-gu, Daejeon 305-701, Republic of Korea. E-mail: shield5200@kaist.ac.kr

[4]Professor, Dept. of Civil and Environmental Engineering, Korea Advanced Institute of Science and Technology (KAIST), Yuseong-gu, Daejeon 305-701, Republic of Korea. E-mail: gyechun@kaist.edu

Note. This manuscript was submitted on July 13, 2013; approved on June 2, 2014; published online on June 27, 2014. Discussion period open until November 27, 2014; separate discussions must be submitted for individual papers. This technical note is part of the ***Journal of Geotechnical and Geoenvironmental Engineering***, © ASCE, ISSN 1090-0241/06014011(4)/$25.00.

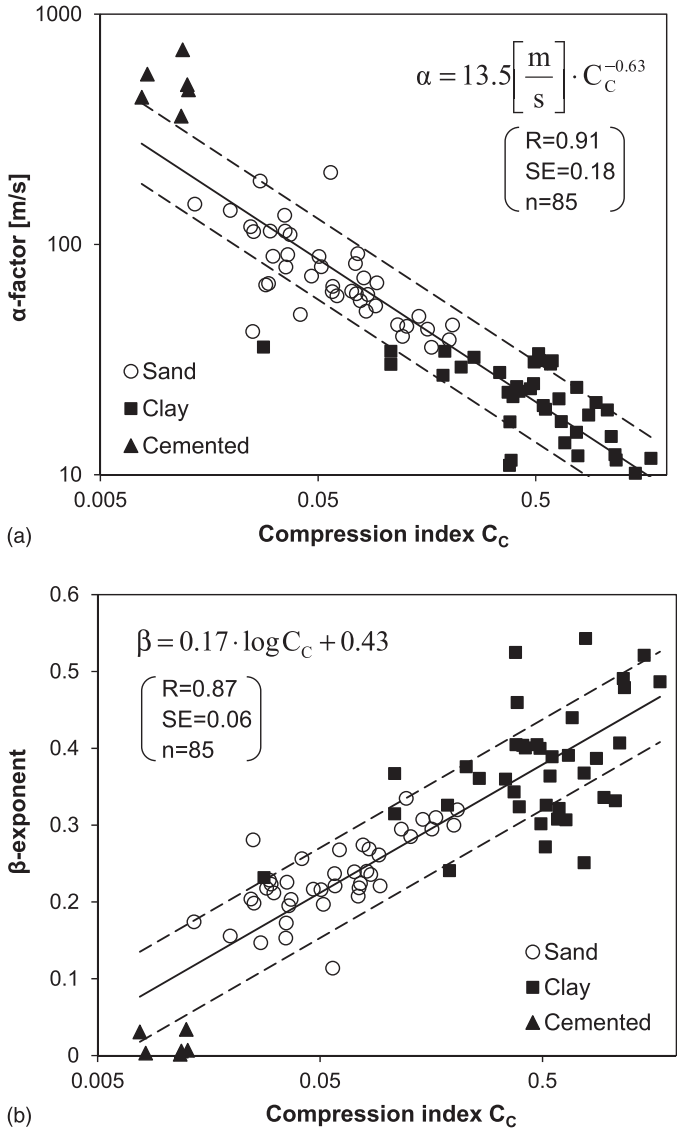

Fig. 1. Relationships between small-strain parameters: (a) α factor (i.e., shear-wave velocity at 1 kPa) and (b) β exponent (i.e., sensitivity of the shear-wave velocity to changes in mean effective stress on the polarization plane) and the sediment compression index C_C (equations define the central trend indicated by the continuous lines; dotted lines define ±1 SD from the central trend)

published by the authors; in most cases, the data were obtained in oedometer cells instrumented with bender elements. All values correspond to stress levels below the yield stress when grain crushing governs sediment compaction. The range of mean effective pressures was from 10 up to 1,200 kPa. In the case of lightly cemented soils, plotted compressibility and velocity parameters were determined before the onset of cementation breakage.

Soils range from lightly cemented dense sands (low C_C, high α, and low β values) to soft, high-specific-surface clays (high C_C, low α, and high β values). It can be observed that highly compressible fine-grained sediments have low shear-wave velocity at low confinement (α factor) and high stiffness sensitivity to changes in mean effective stress on the polarization plane (β exponent). Trends are properly fitted with the following expressions:

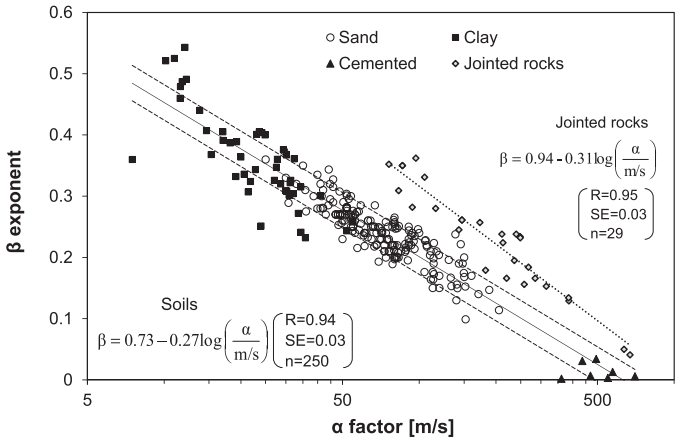

Fig. 2. Inverse relationship between the β exponent and the α factor; data for jointed rocks are shown for comparison (equation defines the central trend for the soil data shown as a continuous line; dotted lines show ±1 SD from the central trend)

$$\alpha = 13.5(\mathrm{m/s})\cdot C_C^{-0.63} \tag{3}$$

$$\beta = 0.17\log C_C + 0.43 \tag{4}$$

Statistical parameters for fitted trends are shown in the figures and include the coefficient of determination R, the standard error (SE), and the number n of data points used in the regression.

The compression index C_C appears in both expressions; this suggests a direct relationship between the α factor (m/s) and the β exponent; combining Eqs. (3) and (4) produces

$$\beta = 0.73 - 0.27\log\left(\frac{\alpha}{\mathrm{m/s}}\right), \quad 1\ \mathrm{m/s} \le \alpha \le \sim 500\ \mathrm{m/s} \tag{5}$$

The database plotted in Fig. 1 and additional data gathered from published studies on wave velocity by other researchers are plotted in Fig. 2. (Note that soil types and all references can be found in Fig. S1 in the Supplemental Data.) The data trend is well predicted by Eq. (5) (superimposed on Fig. 2), which supersedes an earlier relationship that was based on a limited data set [$\beta = 0.36 - \alpha/(700\ \mathrm{m/s})$ in Santamarina et al. (2001)]. Underlying local trends within the full data set presented in Fig. S2 of the Supplemental Data are consistent with differences in compressibility C_C: denser sandy soils, rounder particles, lower plasticity, and higher cementation are associated with higher α factors and smaller β exponents than their counterparts.

Discussion: Physical Interpretation of Observed Trends—Implications

Small- and Large-Strain Stiffness

The tangent-constrained modulus M can be computed from the derivative of Eq. (2), i.e., the local tangent to the e-σ'_z compression curve for a normally consolidated soil

$$M = \frac{d\sigma'_z}{d\varepsilon_z} = 2.3\frac{1+e_0}{C_C}\sigma'_z \tag{6}$$

This is the tangent to a large-strain compressibility trend that involves mostly plastic strains; indeed, the linear dependency with

J. Geotech. Geoenviron. Eng. 2014.140.

vertical effective stress σ_z' underscores the underlying Mohr-Coulomb frictional resistance to deformation. In contrast, the small-strain shear stiffness is a constant-fabric measurement that reflects the stiffness of contacts and follows a power relation with effective stress [Eq. (1)].

α Factor

The small-strain stiffness $E_{\tan}$ of regular arrangements of monosize spherical particles can be computed assuming Hertzian contact behavior; for example, for a simple cubic packing (Richart et al. 1970), see other cases in Santamarina et al. (2001)

$$E_{\tan} = \left[\sqrt[3]{\frac{3}{2}\frac{G_g^2}{(1-\nu_g)^2}}\right]\sigma^{1/3} \tag{7}$$

where G_g and ν_g = shear modulus and Poisson's ratio, respectively, of the mineral that makes the grains. The factor in brackets in Eq. (7) is equivalent to the α factor. The analysis of this and similar expressions for other packings confirms the link between the α factor and grain packing or fabric, as observed in the data (Duffy and Mindlin 1957; Deresiewicz 1974; Petrakis and Dobry 1987; Chang et al. 1991; Santamarina et al. 2001).

β Exponent

The β exponent reflects both the nature of interparticle contacts and fabric changes during loading. Contact deformation at constant fabric can justify the following β values (Cascante and Santamarina 1996):

- $\beta = 0$ for an ideal solid, and $\beta \approx 0$ for cemented granular media (below the transition stress);
- $\beta = 1/6$ for Hertzian contacts (elastic spherical particles);
- $\beta = 1/4$ for cone-to-plane contacts (rough or angular particles);
- $\beta = 1/4$ for particles that experience contact yield; and
- $\beta = 3/4$ for Coulomb's electrical force between charges, and, in general, β is variable with interparticle distance for contacts dominated by double-layer effects.

In addition to contact deformation, data in Fig. 1 show that more compressible soils exhibit a higher β exponent even for the same contact characteristics because of fabric changes and increased coordination number during loading.

Inverse Relationship between α and β

The trend in Fig. 2 is observed from very soft, high-specific-surface soils $\beta \to 0.7$ [e.g., sedimentation from slurry controlled by electrical Coulombian interactions where shear-wave velocities can be as low as $V_s = 0.5$ m/s (data in Klein and Santamarina 2005)] to stiff, lightly cemented sediments where skeletal stiffness exhibits vanishing sensitivity to changes in effective stress $\beta \to 0$ [e.g., lightly cemented sands (Fernandez and Santamarina 2001; Yun and Santamarina 2005)]. For highly cemented sediments, the exponent remains $\beta \approx 0$ in the absence of microfissures or debonding, and the α factor increases with the extent of cementation.

Cementation-Diagenesis-Lithification

The macroscale stiffness estimated for a granular medium where grains interact through Hertzian contacts [Eq. (7)] can be written in terms of the radius of the contact area between grains r_c as

$$\frac{E_{\tan}}{G_g} = \frac{1}{(1-\nu_g)}\frac{r_c}{R} \tag{8}$$

where R = radius of spherical grains. This form of the equation highlights that the sediment skeletal stiffness increases whenever the contact area increases, either from the applied stress (in hertz) or from any diagenetic process such as creep, pressure-solution/precipitation, cementation, and salt precipitation (analyses in Dvorkin et al. 1991; Dvorkin and Yin 1995; Fernandez and Santamarina 2001). Consequently, natural soils tend to be stiffer and less compressible than their remolded counterparts (Dudas 1981; Burland 1990; Abduljauwad and Al-Amoudi 1995; Houston et al. 2001; Herrera et al. 2007). Fully lithified sediments such as shales and sandstones can reach shear-wave velocities as high as 2,500−3,000 m/s. Microfissures can cause stress-dependent stiffness even in lithified sediments, and the exponent may be greater ($\beta \geq 0$).

Preloading

Similar to normally consolidated soils, the small-strain shear stiffness of preloaded sediments is determined by the current state of stress and the void ratio (i.e., interparticle coordination). Changes in the void ratio during loading are only partially recovered during unloading, and residual stresses may remain when zero lateral strain conditions prevail; hence, the void ratio and the horizontal effective stress under k_0 conditions depend on the maximum past pressure σ_p'. Accordingly, several possible predictive equations can be suggested (e.g., Hardin and Black 1969; Houlsby and Wroth 1991; Viggiani and Atkinson; 1995; Shibuya et al. 1997; Vardanega and Bolton 2013).

Jointed Rocks

The shear and longitudinal stiffnesses of jointed rock masses depend on stress resulting from contacts between asperities or between grains that form the gouge material. The global α-β trend for jointed rock masses resembles that for soils, but it is shifted above the soil trend [open rhombuses in Fig. 2; data from Fratta and Santamarina (2002) and Cha et al. (2009)]. Trends within this data set reveal that α increases and β decreases when (1) the stiffness of the intact blocks and the joint separation increase, (2) joint surfaces are rougher, (3) gouge thickness decreases, and (4) the gouge sediment is less plastic [detailed analyses in Fratta and Santamarina (2002) and Cha et al. (2009)].

Engineering Applications

The stiffness of the granular skeleton controls the analysis of deformations in all geosystems, from foundations, tunnels, and pavements to reservoir compaction during oil production. Stress-dependent stiffness adds complexity to such analyses. Causally linked trends reported in this paper can help to discern soil type from velocity-versus-depth profiles (e.g., low α and high β imply high-plasticity clays, high α and low β suggest rounded sands, and $\beta \approx 0$ indicates cemented media), assess the extent of diagenetic cementation ($\beta \to 0$), and preselect and corroborate parameters for analysis. Results show that shear-wave velocity can be used to estimate shear stiffness and compressibility; this is particularly important in aged soils and coarse-grained deposits, where sampling effects and testing difficulties preclude the application of standard testing methods.

Conclusions

The small-strain stiffness of the granular skeleton is a measure of state; it is determined at constant fabric and reflects contact-level deformation.

Shear-wave propagation is a versatile and robust method to determine the small-strain shear stiffness of sediments in the laboratory and the field. The shear-wave velocity follows a power relation with the mean effective stress on the polarization plane $V_s = \alpha(\sigma'_m)^\beta$. The α factor (V_s at $\sigma'_m = 1$ kPa) and the β exponent reflect contact behavior and changes in fabric associated with effective stress changes.

Less-compressible soils exhibit higher α factors and lower β exponents, i.e., clays of lower plasticity, denser sands made of rounder grains, and soils that have experienced diagenetic cementation. There is a robust inverse relationship between α and β for all sediments: $\beta \approx 0.73 - 0.27 \log[\alpha/(\mathrm{m/s})]$. Data for jointed-rock masses agree with the inverse α-β trend, but the data deviate from the trend obtained for sediments.

Acknowledgments

Support for this research was provided by the Department of Energy Savannah River Operations Office (Aiken, South Carolina) and the Goizueta Foundation (Atlanta, Georgia). The authors are grateful to the anonymous reviewers for their valuable comments and insight.

Supplemental Data

Figs. S1 and S2 are available online in the ASCE Library (www.ascelibrary.org).

References

Abduljauwad, S. N., and Al-Amoudi, O. S. B. (1995). "Geotechnical behaviour of saline sabkha soils." *Géotechnique*, 45(3), 425–445.

Burland, J. B. (1990). "On the compressibility and shear strength of natural clays." *Géotechnique*, 40(3), 329–378.

Cascante, G., and Santamarina, J. C. (1996). "Interparticle contact behavior and wave propagation." *J. Geotech. Engrg.*, 10.1061/(ASCE)0733-9410(1996)122:10(831), 831–839.

Cha, M., Cho, G.-C., and Santamarina, J. C. (2009). "Long-wavelength P-wave and S-wave propagation in jointed rock masses." *Geophysics*, 74(5), E205–E214.

Chang, C. S., Misra, A., and Sundaram, S. S. (1991). "Properties of granular packings under low amplitude cyclic loading." *Soil. Dyn. Earthquake Eng.*, 10(4), 201–211.

Deresiewicz, H. (1974). "Bodies in contact with applications to granular media." *R.D. Mindlin and applied mechanics*, B. Herrman, ed., Pergamon Press, New York, 105–147.

Dudas, M. J. (1981). "Long-term leachability of selected elements from fly ash." *Environ. Sci. Technol.*, 15(7), 840–843.

Duffy, J., and Mindlin, R. D. (1957). "Stress-strain relations and vibrations of a granular medium." *J. Appl. Mech.*, 24(11), 585–593.

Dvorkin, J., Mavko, G., and Nur, A. (1991). "The effect of cementation on the elastic properties of granular material." *Mech. Mater.*, 12(3–4), 207–217.

Dvorkin, J., and Yin, H. (1995). "Contact laws for cemented grains: Implications for grain and cement failure." *Int. J. Solids Struct.*, 32(17–18), 2497–2510.

Fernandez, A. L., and Santamarina, J. C. (2001). "Effect of cementation on the small-strain parameters of sands." *Can. Geotech. J.*, 38(1), 191–199.

Fratta, D., and Santamarina, J. C. (2002). "Shear wave propagation in jointed rock: State of stress." *Géotechnique*, 52(7), 495–505.

Hardin, B. O., and Black, W. L. (1969). "Closure of 'Vibration modulus of normally consolidated clay'." *J. Soil Mech. and Found. Div.*, 95(6), 1531–1537.

Hardin, B. O., and Drnevich, V. P. (1972). "Shear modulus and damping in soils: Measurement and parameter effects." *J. Soil Mech. and Found. Div.*, 98(6), 603–624.

Hardin, B. O., and Richart, F. E., Jr. (1963). "Elastic wave velocities in granular soils." *J. Soil Mech. and Found. Div.*, 89(1), 33–65.

Herrera, M. C., Lizcano, A., and Santamarina, J. C. (2007). "Colombian volcanic ash soils." *Characterisation and engineering properties of natural soils*, T. S. Tan, K. K. Phoon, D. W. Hight, and S. Leroueil, eds., Vol. 3, Taylor & Francis, Singapore, 2385–2409.

Houlsby, G. T., and Wroth, C. P. (1991). "The variation of shear modulus of a clay with pressure and overconsolidation ratio." *Soils Found.*, 31(3), 138–143.

Houston, S. L., Houston, W. N., Zapata, C. E., and Lawrence, C. (2001). "Geotechnical engineering practice for collapsible soils." *Geotech. Geol. Eng.*, 19(3–4), 333–355.

Klein, K., and Santamarina, J. C. (2005). "Soft sediments: Wave-based characterization." *Int. J. Geomech.*, 10.1061/(ASCE)1532-3641(2005)5:2(147), 147–157.

Knox, D. P., Stokoe, K. H., and Kopperman, S. E. (1982). "Effect of state of stress on velocity of low-amplitude shear waves propagating along principal stress directions in dry sand." *Technical Rep. GR 82-23*, Geotechnical Engineering Center, Univ. of Texas–Austin, Austin, TX.

Lo Presti, D. C. F., Pallara, O., Costanzo, D., and Impavido, M. (1995). "Small strain measurements during triaxial tests: Many problems, some solutions." *Pre-failure deformation of geomaterials*, S. Shibuya, T. Mitachi, and S. Miura, eds., Balkema, Rotterdam, Netherlands, 1067–1088.

Petrakis, E., and Dobry, R. (1987). "Micromechanical modeling of granular soil at small strain by arrays of elastic spheres." *Rep. No. CE-87-02*, Dept. of Civil Engineering, Rensselaer Polytechnic Institute, Troy, NY.

Richart, F. E., Hall, J. R., and Woods, R. D. (1970). *Vibrations of soils and foundations*, Prentice-Hall, Englewood Cliffs, NJ.

Santamarina, J. C., and Cascante, G. (1996). "Stress anisotropy and wave propagation: A micromechanical view." *Can. Geotech. J.*, 33(5), 770–782.

Santamarina, J. C., Klein, K. A., and Fam, M. A. (2001). *Soils and waves: Particulate materials behavior, characterization and process monitoring*, Wiley, Chichester, U.K.

Shibuya, S., Hwang, S. C., and Mitachi, T. (1997). "Elastic shear modulus of soft clays from shear wave velocity measurement." *Géotechnique*, 47(3), 593–601.

Vardanega, P. J., and Bolton, M. D. (2013). "Stiffness of clays and silts: Normalizing shear modulus and shear strain." *J. Geotech. Geoenviron. Eng.*, 10.1061/(ASCE)GT.1943-5606.0000887, 1575–1589.

Viggiani, G., and Atkinson, J. H. (1995). "Stiffness of fine-grained soil at very small strains." *Géotechnique*, 45(2), 249–265.

Yun, T. S., and Santamarina, J. C. (2005). "Decementation, softening, and collapse: Changes in small-strain shear stiffness in k_0 loading." *J. Geotech. Geoenviron. Eng.*, 10.1061/(ASCE)1090-0241(2005)131:3(350), 350–358.